Urban Climate 24 (2018) 51–62

Contents lists available at ScienceDirect

Urban Climate

journal homepage: www.elsevier.com/locate/uclim

Urban heat islands and cooler infrastructure – Measuring near-surface temperatures with hand-held infrared cameras

Andrew C. Chui[a,f], Alexei Gittelson[b,f], Elizabeth Sebastian[c,f], Natasha Stamler[d,f], Stuart R. Gaffin[e,*]

[a] Boston University, College of Engineering, 44 Cummington Mall, Boston, MA 02215, USA
[b] NASA Goddard Institute for Space Studies, Columbia University, 2880 Broadway, New York, NY 10025, USA
[c] Fusion Academy, 1 MetroTech Center North, Suite 1004, Brooklyn, NY 11201, USA
[d] The Bronx High School of Science, 75 West 205th Street, Bronx, NY 10468, USA
[e] Center for Climate Systems Research & NASA Goddard Institute for Space Studies, Columbia University, 2880 Broadway, New York, NY 10025, USA
[f] NASA Goddard Institute for Space Studies, Climate Change Research Initiative, 2880 Broadway, New York, NY 10025, USA

ARTICLE INFO

Keywords:
Urban heat island
White roofs
Green infrastructure
Surface temperature
Air temperature
Infrared thermography

ABSTRACT

Infrared thermography is an essential tool for evaluating Urban Heat Islands (UHI). Hand-held thermal cameras, however, are only designed for measuring surface temperatures. Near-surface air temperatures are physically different, and although the two temperatures are expected and assumed to correlate, their relationship remains an important research question. It would be a methodological advance if thermal cameras could measure air temperatures too, as it would make mobile data collection more efficient, consistent, and precise. The authors address this by studying the camera temperature readings using a proxy for air temperature – shaded white test-sheets held aloft. The challenge is to minimize near-field absorption of infrared radiation that impinges upon the test-sheets, potentially raising surface temperatures significantly above ambient air temperatures bathing the sheets. The authors correct for the infrared effect using an adjacent sheet of aluminum foil to estimate background radiation impinging on the paper proxy. Results show that at a two-meter height, 86–87% of the measurements closely approximate (within ± 1 °C) of weather station data. Over hotter surfaces, the background infrared test is needed for the proxy temperature reading to be accurate.

1. Introduction

In the effort to mitigate the Urban Heat Island (UHI) effect, which will accompany and reinforce climate change in cities, determining the environmental impacts of different types of infrastructure is a key aspect of research (Corburn, 2009; Wilbanks and Fernandez, 2013). Much of this research has been devoted to the study of cool (e.g. white and green roofs) versus gray (traditional) infrastructure surface temperatures and their implications for urban design and planning policy (Oberndorfer et al., 2007; Rosenzweig and Solecki, 2015). Nonetheless, research gaps remain when discussing how surface temperatures affect proximal and larger-scale air temperatures.

Cool infrastructure refers to any infrastructure that reduces the temperature of surfaces and, presumably, its surroundings, and includes green infrastructure and white roofs. This is important for UHI mitigation strategies. In New York, the CoolRoofs Program

* Corresponding author at: Center for Climate Systems Research & NASA Goddard Institute for Space Studies, Columbia University, 2880 Broadway, New York, NY 10025, USA.
E-mail address: srg43@columbia.edu (S.R. Gaffin).

https://doi.org/10.1016/j.uclim.2017.12.009
Received 11 August 2017; Received in revised form 21 November 2017; Accepted 26 December 2017

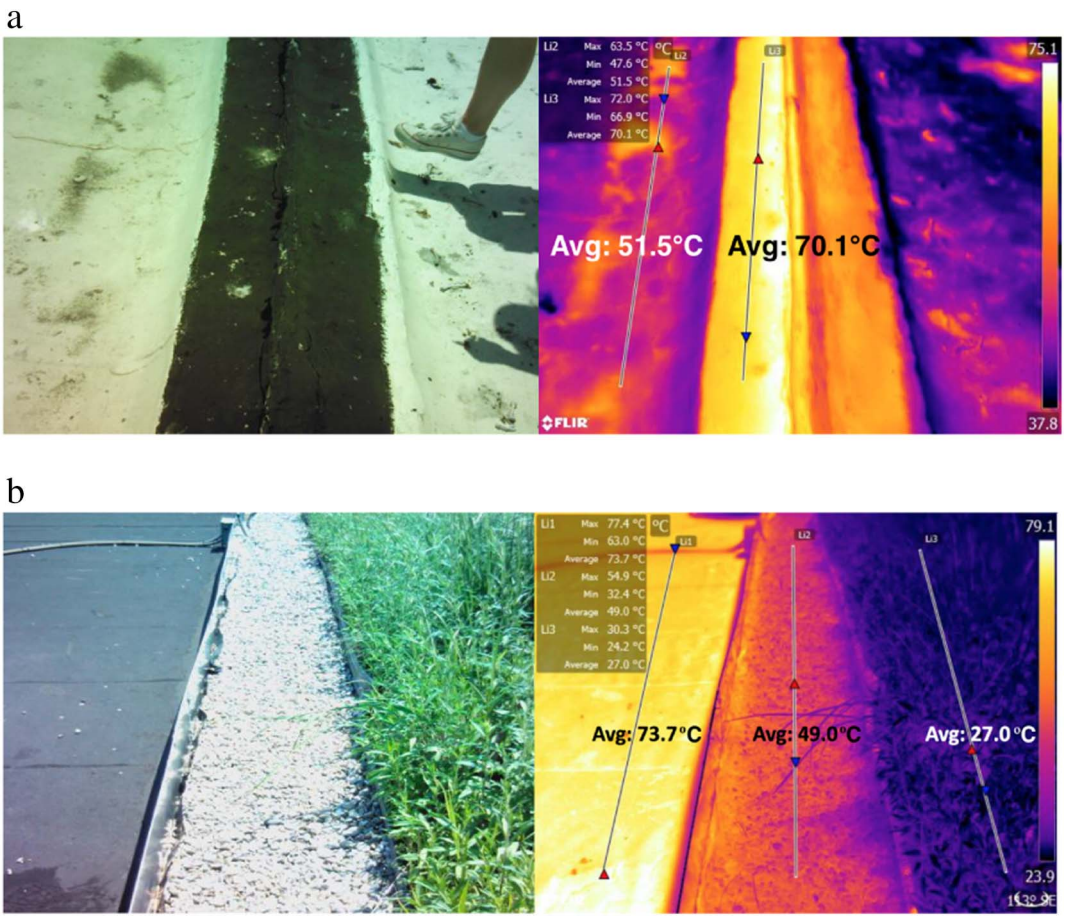

Fig. 1. a. An aged, New York City (NYC) white-paint coated, asphalt roof within the CoolRoofs Program (NYC CoolRoofs, 2017). Average temperatures are shown along measurement lines and comparatively sample the white acrylic elastomeric paint and uncoated black asphalt surface temperatures.
b. A NYC Parks Department green roof. Average temperatures are shown along measurement lines and comparatively sample roof asphalt, rock ballast, and green vegetation. (For interpretation of the references to color in this figure legend, the reader is referred to the web version of this article.)

has coated over 6.6 million ft^2 (613,000 m^2) of building roofs with white reflective paint, and commits to coating at least 1 million ft^2 (93,000 m^2) a year thereafter (Charles-Guzman et al., 2016). Fig. 1 is an example of the typical peak surface temperatures observed on green, white, and dark surfaces. Such temperatures and their differences have frequently been reported and are well-known (Synnefa et al., 2006; U.S. EPA, 2008). Much more challenging are the related questions of what *air* temperature correlations exist with given surface temperature patterns and on what scale?

The study of cool infrastructure's thermal effect on near-surface (1–2 m) air temperature and human comfort is an important component for UHI mitigation (Kruger, 2017). On days where air temperatures rise above 32.2 °C, the mortality rate can increase at least 2% (Carleton and Hsiang, 2016). Certain studies have focused on this issue on a city-wide spatial scale using thermal infrared cameras from high altitudes (Unger et al., 2009), while others have used land-surface temperatures as proxies to estimate the effects on human heat exposure (Ho et al., 2016). Another longitudinal study concluded that outdoor air temperature is a factor in human thermal perception, which led to a predictive formula for estimating these sensory effects (Cheng et al., 2012). However, determining an accurate causal relationship in real-time and at a human scale remains elusive. While some researchers (Nakayoshi et al., 2015a, 2015b) have taken different approaches to understanding the relationship between air temperature, radiation fluxes, and human thermal comfort, our goal here is to use the FLIR sensor imager to as full an extent as possible to measure air temperature using a suitable proxy.

Infrared (IR) cameras (e.g. FLIR, 2017; ICI, 2017) are advantageous for their precision and capacity to collect and process vast amounts of scenic data (pixel-level temperature data), as opposed to air temperature sensors. It would be a methodological advance if thermal cameras could also be used to measure near-surface air temperatures, as it would make data collection more efficient, consistent, and precise. While IR cameras do not measure air temperature directly, it is the goal of this study to ask whether a suitable proxy for this data may be possible using the instrument.

While recognizing that using mobile air temperature probes is the natural first consideration for answering such questions, the authors have frequently attempted this in prior work. However, their experience has been that working with such air probes is not necessarily simpler or provide the needed accuracy. For example, when comparing mobile probes side-by-side, they can differ in their

readings of the same location on the order of degrees, which is the same level of accuracy needed for the air temperature 'signal' expected from cool infrastructure. Usually, introducing different instruments adds to the complexity of the data collection. The FLIR camera may provide greater accuracy and precision than conventional mobile air thermometers. For this study, the authors' assumption is that using a single instrument to take both readings will, with practice, be methodologically simpler than introducing the complication of cross-calibrating two very different instruments - an infrared camera and a mobile air probe temperature sensor.

A simple sheet of white copy paper as a proxy for air temperature using one thermal camera is logical as a first test for this experiment because it has high albedo and is sheer and dry, thus minimizing or eliminating visible light absorption, thermal lags, and latent heat loss.

In this study, a methodology is outlined for this proxy to evaluate air-to-surface relationships, allowing for more effective small-scale analysis of UHI factors. This study focuses on locations in New York City, New York with readily available weather stations in close proximity, specifically Central Park and a rooftop at Columbia University's Lamont-Doherty Earth Observatory.

2. Rationale for study

2.1. Surface temperature versus air temperature

Surface temperatures, also called "radiometric," "brightness," or "skin," temperatures, are determined from longwave radiation emitted by all terrestrial matter (Becker and Li, 1995). These temperatures need to be distinguished, however, from air temperatures, which refer to air parcels near the surface. Air temperature is the more relevant quantity when considering human thermal comfort and seasonal warming and cooling energy demands within buildings (de Dear and Brager, 1998). References to a region's "climate" implicitly mean air temperatures from ground-level weather stations, using a 1.5–2 m elevated, sheltered air temperature sensor.

There are significant temperature differences among different surface materials experiencing the same insolation. Fig. 1a is from a section of a white roof with uncoated black asphalt in the center and white acrylic elastomeric paint on both sides (NYC CoolRoofs, 2017). Albedo loss due to darkening from various sources of soot and rainfall ponding is evident. The original asphalt on the roof is old, and the white paint coating was 3 years old at the time of the image. Fig. 1b shows a section of a green roof with a native grass cover on the right and exposed underlying waterproof asphalt on the left. Between these two areas is a border of white gravel, commonly used for rooftop service access on green roofs. The extreme temperature difference between the dark and white asphalt and vegetation should be noted (> 40 °C). The white gravel, although seemingly of high albedo, is of intermediate temperature, but is still much warmer than vegetation because the gravel is coarse and permits light trapping between the individual rock surfaces (Gruzen Samton Architects LLP, 2007). The low temperature on the vegetated surface, in this example, is due to evapotranspiration (ET). Indeed, this data indicates that without ET thermo-regulation, plant temperatures would likely reach levels that would cause them to perish.

Although surface and associated near-surface air temperatures may be correlated, in general, they should not be equated. For example, during the daytime, in strong sunlight, surface temperatures are generally much higher than nearby air temperatures, but during the night, they are often much lower. For the purpose of urban heat island mitigation, reducing the surface temperature also reduces the lowermost boundary layer of air temperature via convective heating from below (Oke, 1987; Bowler et al., 2010).

Fig. 2 shows remote sensing IR temperature data taken at a 60-meter spatial resolution as retrieved on August 14, 2002 at 10:30 AM, along with selected visual site imagery at major UHI hotspots. The figure illustrates some of the main factors leading to high urban surface temperatures on a large scale. These include low-albedo surfaces, absence of vegetation, solar incidence angle relative to a surface, and light trapping, supporting the techniques mentioned as first-order approaches to UHI mitigation.

2.2. The challenge of measuring air and surface temperature correlations

Ultimately, some of the most significant UHI mitigation questions are still unanswered, such as:

- What air temperature correlations exist with given surface temperature patterns and on what scale, including large scales?
- With even the most ambitious surface temperature reduction programs in cities, including extensive urban forestry and complete flat rooftop conversion to white roofs, what overall (e.g. annual) air temperature reduction can be expected?

For example, Fig. 3 demonstrates the immediate surface temperature reductions achievable with a high-albedo modification of a dark asphalt roof, using, in this example, the simple technique of applying white acrylic elastomeric paint to the waterproof membrane. This simple low-cost method is one of the cornerstone UHI mitigation programs currently ongoing in New York City and other cities as well (Takebayashi and Moriyama, 2007). But if all flat roofs in an urban area – which cumulatively often comprise about 20% of urban land area (EPA, 2008) – were transformed to high-albedo, how much reduction can be expected in overall annual urban air temperature?

2.3. The challenge of measuring urban air cooling

To illustrate the challenge of measuring surface-air temperature correlations, Fig. 4 shows an ultimately successful correlation between surface temperatures and air temperatures for a daytime transverse through New York City's Central Park using common hand-held air temperature probes (e.g. ThermoWorks, 2017; PCE, 2017; Fluke, 2017). However, this seemingly obvious correlation

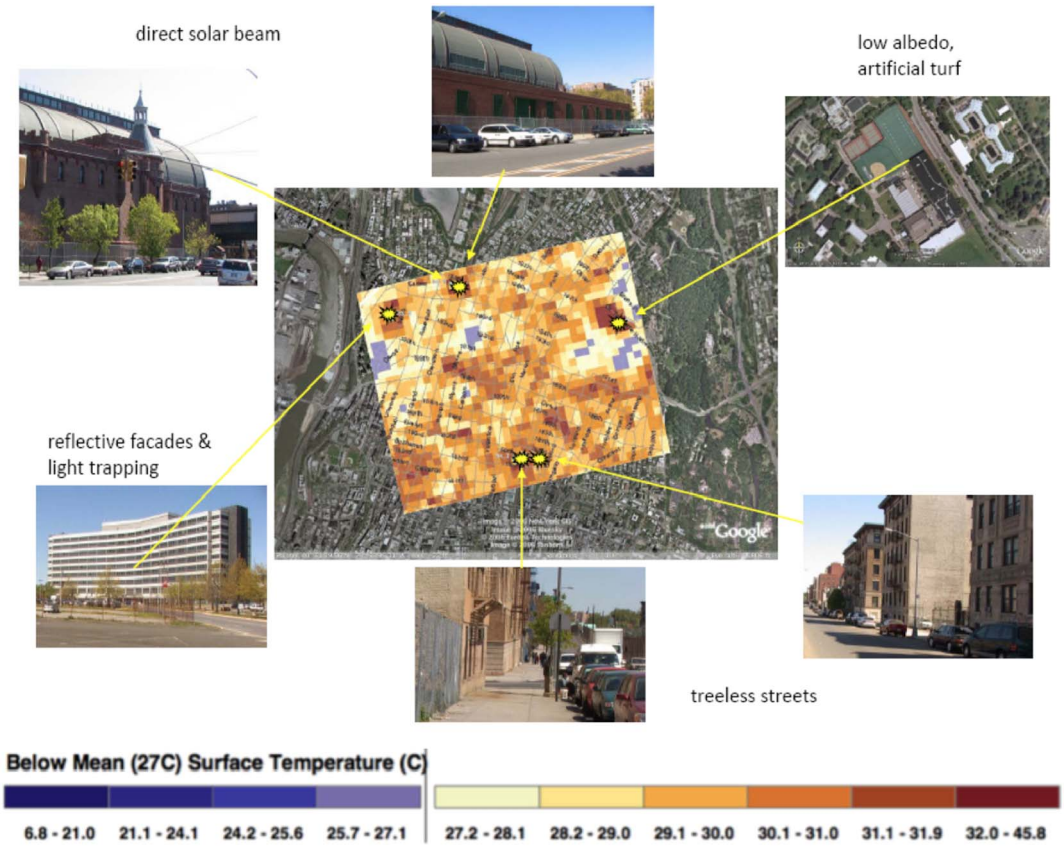

Fig. 2. Visual urban imagery overlaid with a NASA Landsat 7 temperature map, highlighting areas of high surface temperature located in the Fordham area, Bronx, New York (Gaffin et al., 2017).

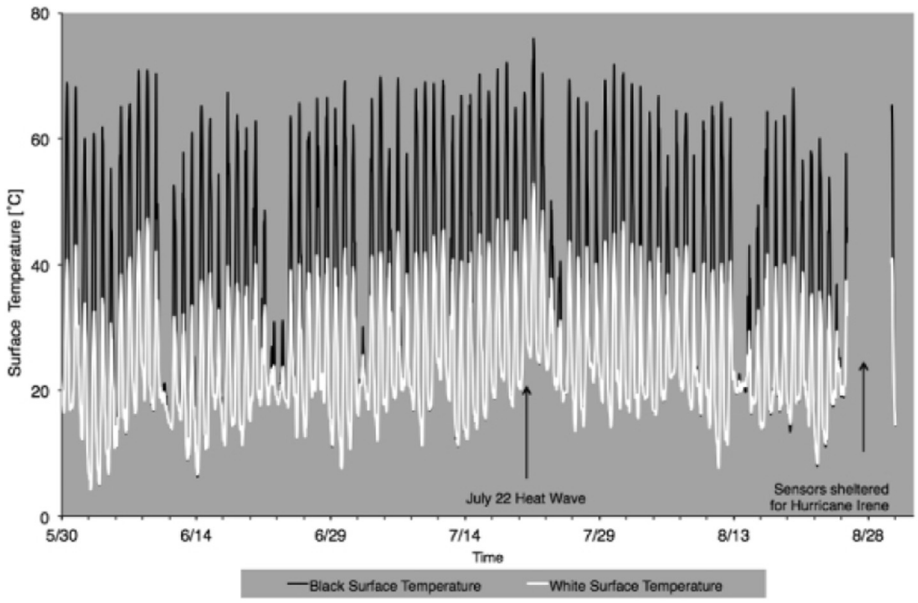

Fig. 3. Comparative high- and low-albedo roof temperatures at Museum of Modern Art Queens (Long Island City, New York), where white acrylic paint (high albedo) was partially applied to a black asphaltic substrate (low albedo). Data shown is for June–August 2011, collected by Center for Climate Systems Research (Gaffin et al., 2012).

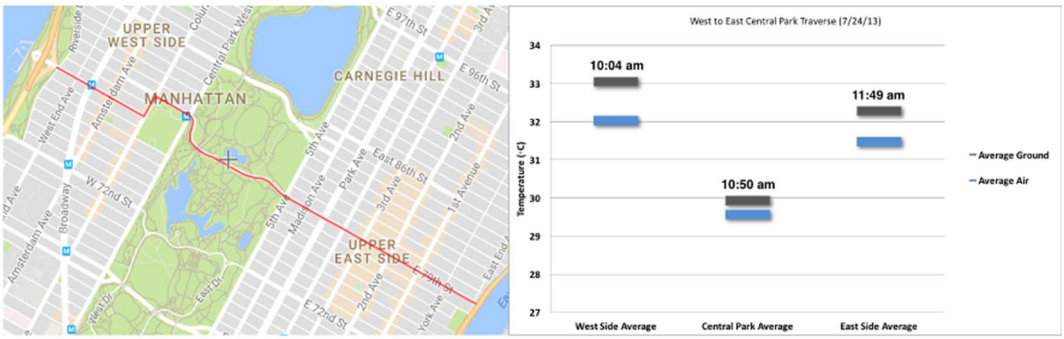

Fig. 4. Previous Central Park transverse air and ground temperature experiment readings. Shown are observed ground and associated air temperatures using the air temperature (non-IR) probes and spot sensors (ThermoWorks, 2017).

took many attempts and was only detectable with broad sampling of the streets surrounding the park, so smaller scale green infrastructure air temperature benefits would be even more difficult to detect.

In a controlled indoor experiment where the air temperature was regulated with a space heater, two different air probes placed at the same spot indicated two different readings, confirming suspicions about inconsistent readings outdoors using these handheld probes. In other words, if a city's largest green infrastructure areas, like urban parks, are challenging for such an experiment, smaller scale greening projects like greenstreets, street tree programs, and bioswales would be even more difficult.

Using IR thermography and a proxy to measure these readings could be more beneficial than using current air temperature sensors by providing a greater amount of data with greater accuracy. If the proxy proves to measure the relative local temperature of air in addition to measuring surface temperature, the relationship between the two could be studied in greater detail.

3. Methods

3.1. Site areas

The study was conducted in the greater New York City area and data were collected at two locations: (i) the National Weather Service NOAA Central Park weather station (designation KNYC); and (ii) the Columbia University Lamont-Doherty Earth Observatory (LDEO) weather station (designation KNYPALIS3).

The Central Park station is located just south of the 79th Street Transverse (Fig. 4) and uses an automated surface observing system (ASOS) as well as three Thermometrics Corp. PT1000 platinum resistance thermometers housed in fan-aspirated solar radiation shields (NCEI, 2017). The station is situated in a tree-shaded area of the park and is surrounded by green, almost forested landscape.

The second site was the weather station at the Columbia University Lamont-Doherty Earth Observatory located in Palisades, New York. The station consists of a Davis Vantage Pro2 using a p-n junction silicon diode sensor. Its temperature sensor accuracy is ± 0.3 °C (Davis Inst., 2017). The LDEO station provides a contrasting environment to the Central Park station and was indicative of an urban gray infrastructure environment. It is situated atop a roof, which is composed of asphalt and has an unobstructed 360° view of the surrounding area, which includes other research buildings and asphalt parking lots.

Thus, it was assumed that the Central Park site approximateed urban green infrastructure while the LDEO site will approximate urban gray infrastructure. Measurements were taken during similar weather conditions.

3.2. Thermographic camera and proxy

The experiment was conducted using a FLIR T650sc infrared camera (FLIR, 2017). It has a high sensitivity and can measure temperatures to within 1 °C at a 0.001° resolution (FLIR, 2017). The instrument and software also have extensive data and graphical processing capacity not similarly available with air temperature sensors.

In developing a proxy, the general goal is to minimize all energy impingement or flux that would affect the resulting proxy surface temperature, other than the surrounding air temperature that it is bathed in. Whiteness ensures high albedo and thus minimizes shortwave absorption. The fact that no moisture is present on the sheet ensures the lack of ET and thus no latent heat cooling.

Experiments were conducted among a few choices for the test proxy to determine which provides closest agreement to actual air temperatures. Standard copy paper, white foam core, and white construction (“heavy”) paper were included.

Results in Fig. 5 show that all materials tested well and were accurate within 0.5 °C of the weather station air temperature reading. The foam core and heavy paper temperatures were not sensitive to different heights, suggesting a temporal lag. Copy paper showed temperature variability consistent with different heights, suggesting a quick response time without temporal lags.

The paper proxy alone, however, does not account for the more difficult factor of potential IR absorption from surrounding near-field sources, such as the nearby hot ground or buildings.

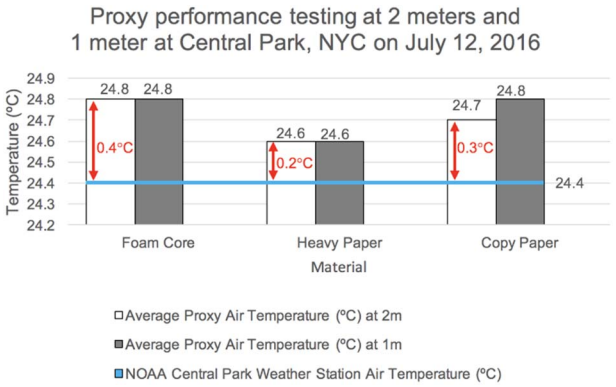

Fig. 5. Results on performance levels at different heights of various white materials (foam core, heavy white paper, and copy paper) against official air temperature readings from the NOAA Central Park weather station.

3.3. Aluminum foil reflected temperature proxy

To determine the near-field reflected temperature impacting the paper proxy from surrounding surfaces, a sheet of aluminum foil was used and placed adjacent to the paper proxy. Reflected temperature can be defined as the temperature of the energy incident upon the surface of a specimen (ASTM, 1997). The user-supplied camera reflected temperature was set at the atmospheric temperature, and the emissivity was set to the emissivity of white copy paper: 0.9. The foil represents near-perfect infrared reflection (pure reflection is an emissivity of 0, aluminum foil has an emissivity of 0.04). By setting the camera for this near-perfect reflector to an emissivity of 0.9, the same emissivity as the copy paper, it should measure the reflected infrared energy onto the proxy.

The easy crinkling of aluminum foil led to large temperature variation across one sheet of foil (the peaks and canyons in the foil reflect light in different angles, causing the camera to interpret different surface temperatures), so the average temperature reading was used for the copy paper proxy in subsequent trials. The aluminum foil is considered a good proxy for reflected temperature because: (i) it has a very low emissivity (0.04); (ii) it is thin, preventing heat from being stored; (iii) it is inexpensive and accessible like copy paper.

3.4. Data collection methods

The physical equipment setup is shown in Fig. 6. To avoid human thermal interference, a hand-held wooden boom was attached to a white rigid frame holding the test sheets in place. In addition to using high-albedo test sheets, the proxy was shaded with an umbrella to block sunlight from above.

The images were captured between the hours of 11:00 AM and 3:00 PM on clear days. First, reflected temperature was adjusted using the aluminum foil test. Then, ten trials of images were collected. In each trial, 5 images were taken for two different heights: 1 m and 2 m. In all trials, measurements were taken 2 m away from the weather station.

Proper parameter setting for the camera was essential for accurate imaging; including atmospheric temperature, humidity, emissivity, and reflected temperature. The first two were based on proximate weather station data; emissivity was set at 0.9 based on research and manufacturer recommendation for white copy paper. The reflected temperature compensated for temperatures from surrounding objects reflecting onto the proxy and was obtained from the aluminum foil test (Orlove, 2013).

3.5. Data extraction

Data were extracted using FLIR Tools software, including maximum, minimum, and average temperatures for a selected region, and further extracted into an Excel file. The data are in the form of temperature readings captured by each pixel. Each image contains about 236,000 of temperature data points. These are the raw data of the images, which FLIR Tools organizes for ease of use. For the images, the data points of interest were the temperature readings confined to the test sheet area alone (Fig. 6b).

4. Results

4.1. Central Park

Ten trials consisting of five images each were taken at 1 and 2 m (totaling 100 images), and comparisons to one minute time-step temperature readings confirmed our observations. Recordings within trials were fairly comparable. An interesting trend observed during analysis was warming as height increased and attributed to the ET cooling of the plants towards the bottom of the proxy, which was closer to the ground.

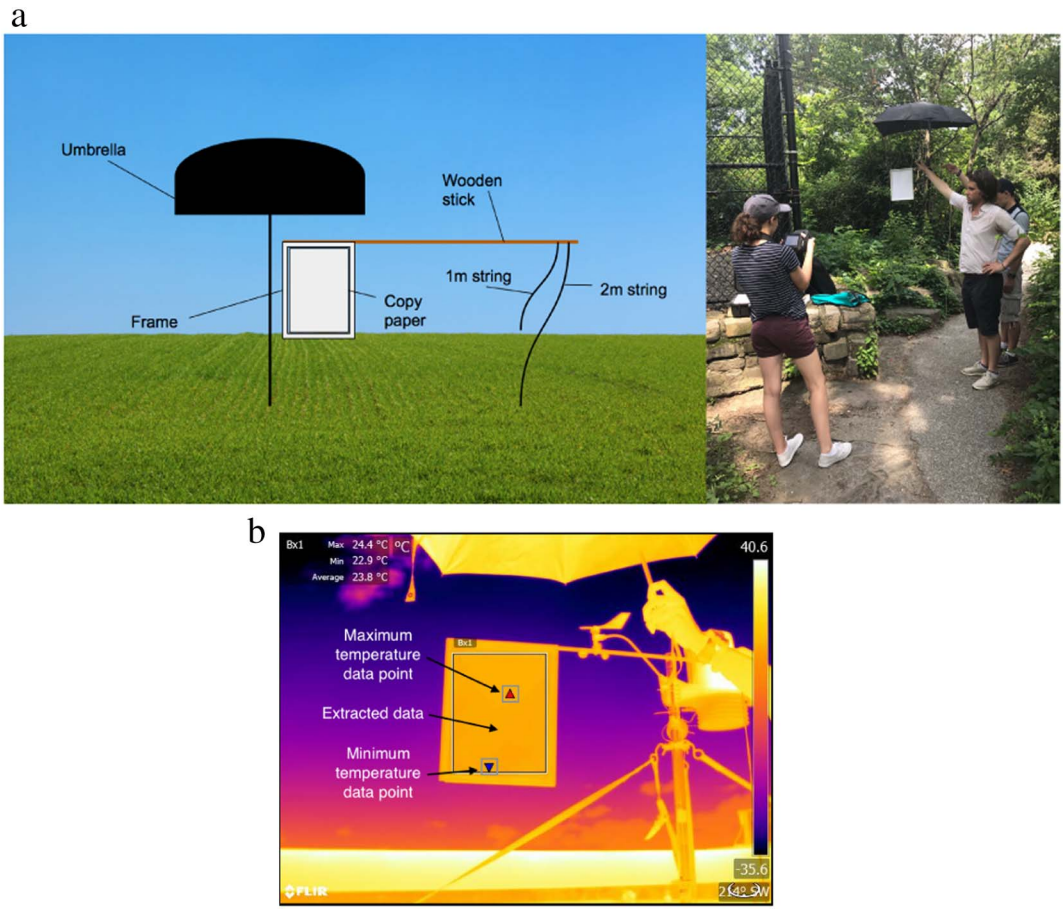

Fig. 6. a. Experimental set-up: an umbrella was held over the proxy to shield from sunlight; a wooden boom maintained distance between the person and proxy; set-up was held at heights of 1 m and 2 m; measurements were taken 2 m away from the weather station.
b. Experimental set-up shown in the IR spectrum using the FLIR Tools analysis software, and sample of extracted temperature data.

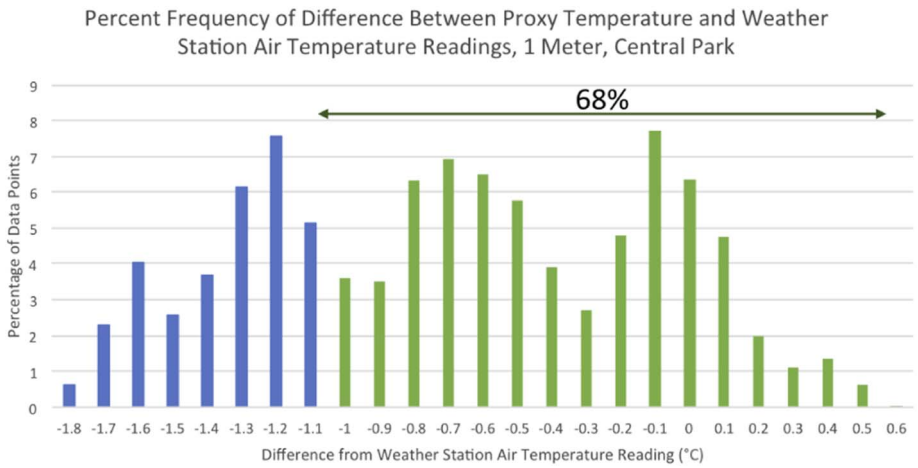

Fig. 7. Represents the percentage of data points and their difference from Central Park weather station data at 1 m. The green section represents the overall percentage within the ± 1 °C range. Positive x-axis values represent readings higher than the weather station air temperature, while negative x-axis values represent readings lower than the weather station air temperature. (For interpretation of the references to color in this figure legend, the reader is referred to the web version of this article.)

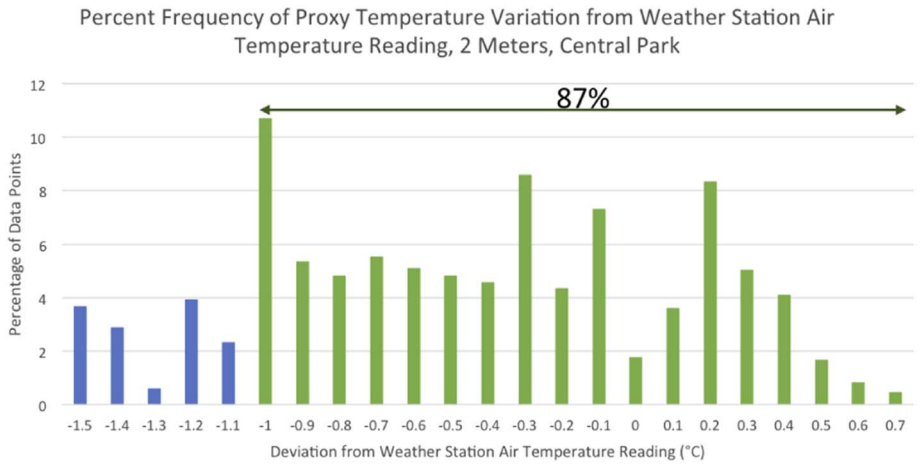

Fig. 8. Represents the percentage of data points and their difference from Central Park weather station data at 2 m. The green section represents the overall percentage within the ± 1 °C range. Positive x-axis values represent readings higher than the weather station air temperature, while negative x-axis values represent readings lower than the weather station air temperature. (For interpretation of the references to color in this figure legend, the reader is referred to the web version of this article.)

4.1.1. Distance from ground surface: 1 m (Fig. 7)

4.1.2. Distance from ground surface: 2 m (Fig. 8)

Recordings at 2 m were far more accurate in comparison to recordings at 1 m.

4.2. Lamont-Doherty Earth Observatory (LDEO) testing

The same methods were used at LDEO as at Central Park. One minute data updates were provided by the weather station. A trend observed during analysis was cooling as height increased and was attributed to the convection of heat rising from the hot ground surface and warming the bottom of the proxy.

4.2.1. Distance from ground surface: 1 m (Fig. 9)

4.2.2. Distance from ground surface: 2 m (Fig. 10)

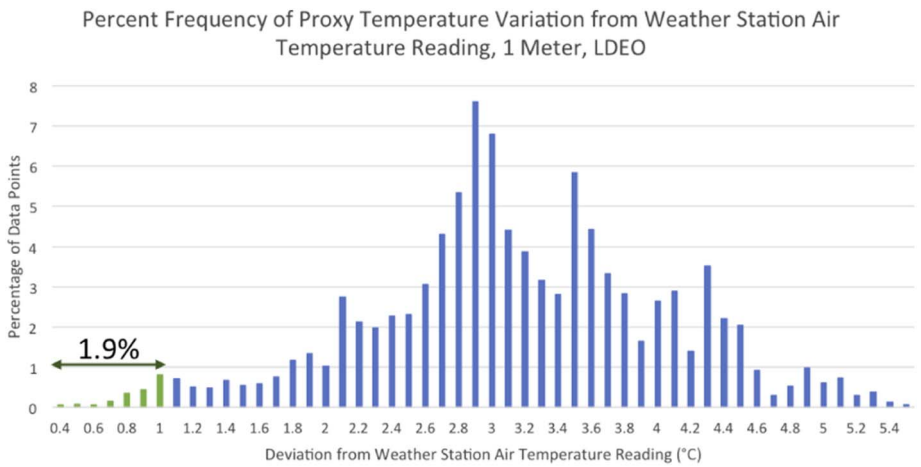

Fig. 9. Represents the percentage of data points and their difference from LDEO weather station data at 1 m. The green section represents the overall percentage within the ± 1 °C range. Positive x-axis values represent readings higher than the weather station air temperature, while negative x-axis values represent readings lower than the weather station air temperature. (For interpretation of the references to color in this figure legend, the reader is referred to the web version of this article.)

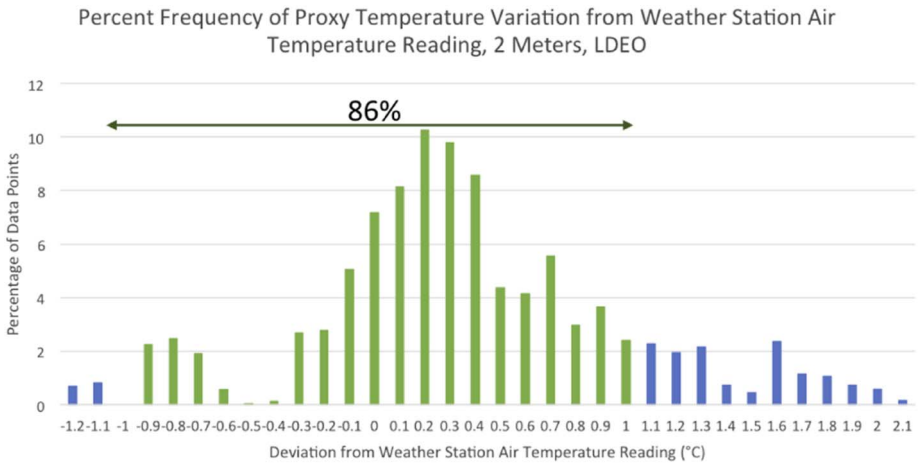

Fig. 10. Represents the percentage of data points and their difference from LDEO weather station data at 2 m. The green section represents the overall percentage within the ± 1 °C range. Positive x-axis values represent readings higher than the weather station air temperature, while negative x-axis values represent readings lower than the weather station air temperature. (For interpretation of the references to color in this figure legend, the reader is referred to the web version of this article.)

5. Discussion

With this new methodology for measuring air temperatures using IR cameras, determining and defining proxy data accuracy (as compared to weather station data) is necessary. FLIR IR cameras can measure temperatures with a spatial resolution of 0.001° (FLIR, 2017) and makes them sensitive to relative temperature changes within the proxy, which was useful in recognizing the potential effect of convection from the roof at LDEO onto the proxy.

5.1. Comparison to thermal comfort standards

According to the Handbook of Air Conditioning and Refrigeration, a tolerance of ± 1.1–1.7 °C is considered acceptable in cases of human thermal comfort (Wang, 2001). According to the international standard ISO 7726, the acceptable accuracy required for measurements is ± 0.9 °C (ISO, 1998).

In terms of human thermal comfort, if temperature is increasing at a slow pace of 0.5 °C per minute, people usually do not detect a rise in temperature until the change is > 5 °C (Jones, 2009). This signifies that the accuracy of instrumentation is greater than that of people, and therefore humans would not notice the difference that the measurements are detecting. 1 °C was therefore determined to be an appropriate compromise between the thermal comfort tolerance and the international standard for device accuracy. Over 85% of the data at 2 m are within this range.

Measurement of reflected temperature became an issue during testing. Initially, the reflected temperature was set to the same value as the atmospheric temperature, which would make sense theoretically, given that the air behind the camera should be the same temperature as the air in front of the camera. However, this is not an accurate assumption, given that a person is typically behind the camera along with other environmental factors. There are also the effects of surfaces behind the camera impacting the area and causing elements such as air to have higher temperatures than reported by the weather station.

5.2. Comparison of data

The data collected by the IR camera from each site were compared to those of each respective weather station. The average temperature of the entire proxy should theoretically be able to be compared to the weather station to determine the accuracy of the proxy. The relationship between the data collected and the weather station data shows how accurate the proxy can be.

Additionally, an interesting aspect is how much data can be extracted from the surface of the proxy along with the multitude of ways it can be organized. This is explained by the fact that the proxy is not one uniform temperature. One way is to represent the change through graphs, showing the spot temperature breakdown of the paper itself. This shows how temperatures vary over height and the possible heat transference over distance. Both sites exhibit this trend, but the direction of the trends is opposite.

Over green infrastructure, the hotter temperatures were closer to the top of the page. This is indicative of the cooling effect of plants due to ET. The data from LDEO has the opposite trend, where the hottest parts of the paper are on the bottom. This is indicative of the convective heat from the ground surface affecting the temperature of the proxy. Both of these trends can be used to determine the effects that different surfaces have on the air temperatures above them.

5.3. Comparison to other methods

5.3.1. Weather stations

The difference in these temperatures lies within the instruments used. Traditionally, air temperature is gathered by air temperature sensors on weather stations. The Central Park weather station is NOAA regulated and has a Thermometrics Corp. PT1000 platinum resistance thermometer. These NOAA weather stations are the standard for weather data, which includes temperature measurements. The LDEO weather station is a Davis Vantage Pro2 model with an p-n junction silicon diode air temperature sensor that measures with an accuracy of ± 0.3 °C. This methodology seeks to prove that thermal imaging using a proxy is similarly effective at measuring air temperature. While not as accurate, the results seem to justify that it is suitable for measuring these temperatures. The unique aspect of using IR images to capture thermal data is that air temperature is not being measured directly, rather it is being measured indirectly through the use of a proxy. Through the use of this new methodology, experiments can be conducted to simultaneously compare air temperature to surface temperatures.

5.3.2. IR guns

One of the most common portable methods for measuring air temperature is an IR gun with an air probe, such as the ThermoWorks Industrial IR Gun (IR-GUN-S) with the ThermoWorks plug-mount air/gas probe (− 301). This IR gun has an accuracy of 2 °C between 0 °C and 550 °C and a resolution of 0.1° from − 9.9 to 199.9, less than the IR camera. There are a few issues with IR guns. First, IR guns are meant to take spot measurements, so they only give one temperature measurement within the spot range. Each IR gun has a different distance-target spot ratio (D-S ratio), ranging for 1:1 to 60:1 for higher end models, so they have different spot ranges. The ThermoWorks Industrial IR Gun, for example, has a D-S ratio of 12:1, which means that it measures an approximately one-inch diameter spot when 12 in away from the target object (about a 2.5 cm spot when 30 cm away from the target). This creates two scenarios.

The first scenario is that the whole proxy is in the view range of the IR gun. In this case, the gun will only report one temperature for the entire sheet of paper, which prevents recognition of variations in temperature throughout the paper, a trend recognized by the IR camera. Additionally, as its spot size increases, the accuracy of the gun's temperature reading decreases, so creating a spot that encompasses the entire 8.5″ × 11″ sheet of paper would introduce a significant degree of inaccuracy.

The second scenario is that only part of the proxy is in the view range of the IR gun to maximize accuracy. This forces the spot size to be small to a degree that is not representative of the sensitivity of human skin. A one- or two-inch diameter spot is not what is felt by the entire core of the body, especially if there is a significant temperature gradient. To realize a temperature gradient or accurately demonstrate the temperature of the full core of the body, many spot measurements would have to be taken, which is time-consuming and impractical.

Both of these scenarios are avoided with the IR camera. The camera is meant to capture an entire image and comes with software, such as FLIR tools, that allows for the extraction of smaller areas of data. Each pixel of the camera image functions as an IR gun spot, providing thousands of points in one image that are each more accurate than a spot temperature from the IR gun.

5.3.3. Remote sensing

Remote sensing via satellite is another form of prevalent measurement techniques. Both NASA and NOAA satellites analyze temperature data, but the degree of accuracy of each is different in scale to the techniques measured above. These remote sensing satellites measure the surface temperatures, and the ones that measure air temperature calculate it based off the radiation emitted by gases in the atmosphere (National Research Council, 2000). While these satellites are very accurate for what they do, they still lack the close-up accuracy that other methods provide. The best resolution these satellites can get is about 30 m per pixel. Ground based techniques can give the temperature based on their exact location, which is much more beneficial when trying to determine local spot temperatures.

5.4. Possible field applications

Given the prior approaches to measure the air temperature above these surfaces, this methodology could be used in the field to help measure near surface temperatures of various infrastructures. This more accurate and adaptable method could be applied to obtain field measurements over various green infrastructure at small scales as depicted in Section 3.4. More measurements still need to be taken using this methodology with the proxy. As discussed in the introduction, mobile air sensors will be further tested for comparison. In the future, the camera and proxy could be used to simultaneously find both surface and air temperatures, thereby reducing the number of instruments needed for cross calibration. The method could potentially assist policymakers and city planners to improve the design of urban spaces.

6. Conclusions

The study of air-to-surface temperature relationships is important for urban climate research. Evaluating the nature of these relationships at a small scale (< 30-meter surface areas) is especially important for understanding how green and gray infrastructure affect the urban heat island, thermal comfort, and building energy use. Portable thermal cameras may allow for a precise and effective way to measure near-surface air temperatures.

This study performed thermal imaging tests using white copy paper as a proxy for measuring these air temperatures by comparing

it to weather station data in two different types of locations. On one hand, it is possible to conclude that, at a height of 2 m, white copy paper is an appropriate material to further test influences of surfaces on air. Taking into account reflected temperature as one of the parameters is key to obtaining more precise proxy temperature measurements. On the other hand, at a height of 1 m, the methodology was ineffective at measuring air temperature, although it performed significantly better over green infrastructure.

We understand this approach is an approximation but looking at the temperatures on a very small scale is still difficult, as seen in the results from the Columbia rooftop. We acknowledge and understand there needs to be a great deal more testing that needs to be done using the proposed methodology. We need to conduct further analysis of external factors such as reflected temperature from surrounding objects and their effects on the proxy and camera's measurements. Ultimately, the goal is to come up with better and more strategically placed urban heat island interventions such as green infrastructure.

Acknowledgments

This research was supported by the National Science Foundation (NSF) Coastal SEES Award #1325676. Any opinions, findings, and conclusions expressed in this letter are those of the authors and not meant to represent the views of any supporting institution. We would also like to thank the New York City Mayor's Office of Recovery and Resiliency for use of the FLIR thermal imaging cameras. Further support was provided by NASA's Office of Strategic Infrastructure, NASA's Science Mission Directorate (SMD), NASA Goddard Institute for Space Studies (GISS), NASA Goddard Space Flight Center (GSFC) Office of Education 160, NASA Climate Change Research Initiative (CCRI), and the Universities Space Research Association (USRA). K. Byrd, C.D. Herrera, and G. Kim contributed to early data collection and processing. We additionally would like to thank D.Ng for helping in the process of the assembly and revision of the manuscript.

References

American Society for Testing and Materials (ASTM), 1997. Standard Test Methods for Measuring and Compensating for Reflected Temperature Using Infrared Imaging Radiometers. Active Standard ASTM E1862. http://www.irss.ca/development/documents/CODES%20&%20STANDARDS_02-28-08/ASTM/Thermography/Test%20Method%20for/E1862-97%20Infrared%20Imaging%20Radiometers.pdf, Accessed date: August 2017.

Becker, F., Li, Z.L., 1995. Surface temperature and emissivity at various scales: definition, measurement and related problems. Remote Sens. Rev. 12 (3–4), 225–253. http://dx.doi.org/10.1080/02757259509532286.

Bowler, D., Buyung-Ali, L., Knight, T., Pullin, A., 2010. Urban greening to cool towns and cities: a systematic review of the empirical evidence. Landsc. Urban Plan. 97 (3), 147–155. http://dx.doi.org/10.1016/j.landurbplan.2010.05.006.

Carleton, T.A., Hsiang, S.M., 2016. Social and economic impacts of climate. Science 353 (6304) 1112-aad9837-15. https://doi.org/10.1126/science.aad9837.

Charles-Guzman, K., Fuhlbrugge, L., Hugens, D., Namgyal, N., Onwufor, R., Radhakrishnan, S., Scott, M., Seed, B.J., Takaki, M.S., Trushell, D.A., Valdivieso, J.P., Williams, L., El Yamani, S., Zill, Z., 2016. Strategic Guidance for the NYC CoolRoofs Program, 2017–2018. The Earth Institute Columbia University. http://sustainability.ei.columbia.edu/files/2013/05/NYC-CoolRoofs-Capstone-Final-Report.pdf, Accessed date: August 2017.

Cheng, V., Ng, E., Chan, C., Givoni, B., 2012. Outdoor thermal comfort study in a sub-tropical climate: a longitudinal study based in Hong Kong. Int. J. Biometeorol. 56 (1), 43–56. http://dx.doi.org/10.1007/s00484-010-0396-z.

Corburn, J., 2009. Cities, climate change and urban heat island mitigation: localising global environmental science. Urban Stud. 46 (2), 413–427. http://dx.doi.org/10.1177/0042098008099361.

Davis Instruments, 2017. Cabled Vantage Pro2 & Vantage Pro2 Plus Stations. Spec Sheet. https://www.davisnet.com/product_documents/weather/spec_sheets/6152C_6162C_SS.pdf, Accessed date: August 2017.

de Dear, R., Brager, G.S., 1998. Developing an adaptive model of thermal comfort and preference. ASHRAE Trans. 104 (1a), 145–167. http://www.cbe.berkeley.edu/research/other-papers/de%20Dear%20-%20Brager%201998%20Developing%20an%20adaptive%20model%20of%20thermal%20comfort%20and%20preference.pdf, Accessed date: August 2017.

FLIR, 2017. FLIR T600-Series Infrared Camera. http://www.flir.com/science/display/?id=46818, Accessed date: August 2017.

Fluke, 2017. Fluke 561 Infrared and Contact Thermometer. http://en-us.fluke.com/products/thermometers/fluke-561-thermometer.html, Accessed date: August 2017.

Gaffin, S.R., Imhoff, M., Rosenzweig, C., Khanbilvardi, R., Pasqualini, A., Kong, A.Y.Y., Grillo, D., Freed, A., Hillel, D., Hartung, E., 2012. Bright is the new black: multi-year performance of high-albedo roofs in an urban climate. Environ. Res. Lett. 7, 014029. http://dx.doi.org/10.1088/1748-9326/7/1/014029.

Gaffin, S.R., Kong, A.Y.Y., De Mel, J.M., Rosenzweig, C., 2017. Green, White, and Dark Roofs: The Energy Perspective. Columbia University Center for Climate Systems Research and NASA Goddard Institute for Space Studies.

Gruzen Samton Architects LLP, 2007. DDC Cool & Green Roofing Manual. http://www.nyc.gov/html/ddc/downloads/pdf/cool_green_roof_man.pdf, Accessed date: August 2017.

Ho, C.H., Knudby, A., Xu, Y., Hodul, M., Aminipouri, M., 2016. A comparison of urban heat islands mapped using skin temperature, air temperature, and apparent temperature (Humidex), for the greater Vancouver area. Sci. Total Environ. 544, 929–938. http://dx.doi.org/10.1016/j.scitotenv.2015.12.021.

Infrared Cameras Inc. (ICI), 2017. T-Cam 80 P-Series|Handheld Thermal Camera with Temperature Measurement. http://www.infraredcamerasinc.com/shop/products/t-cam-80-p-series, Accessed date: August 2017.

International Organization for Standardization (ISO) 7726, 1998. Ergonomics of the Thermal Environment – Instruments for Measuring Physical Quantities. https://www.iso.org/obp/ui/#iso:std:iso:7726:ed-2:v1:en, Accessed date: August 2017.

Jones, L., 2009. Thermal touch. Scholarpedia 4 (5), 7955. revision #149555. https://doi.org/10.4249/scholarpedia.7955.

Kruger, E., 2017. Impact of site-specific morphology on outdoor thermal perception: a case-study in a subtropical location. Urban Clim. http://dx.doi.org/10.1016/j.uclim.2017.06.001.

Nakayoshi, M., Kanda, M., de Dear, R., 2015a. Globe anemo-radiometer. Bound.-Layer Meteorol. 155 (2), 209–227. http://dx.doi.org/10.1007/s10546-014-0003-7.

Nakayoshi, M., Kanda, M., Shi, R., de Dear, R., 2015b. Outdoor thermal physiology along human pathways: a study using a wearable measurement system. Int. J. Biometeorol. 59 (5), 503–515. http://dx.doi.org/10.1007/s00484-014-0864-y.

National Research Council (U.S.). Committee on Earth Studies, 2000. "Atmospheric Soundings". Issues in the Integration of Research and Operational Satellite Systems for Climate Research: Part I. Science and Design. National Academy Press, Washington, D.C, 0-309-51527-0pp. 17–24.

National Centers for Environmental Information (NCEI), 2017. Instruments. U.S. Climate Reference Network. https://www.ncdc.noaa.gov/crn/instruments.html, Accessed date: August 2017.

NYC CoolRoofs, 2017. NYC CoolRoofs. https://www1.nyc.gov/nycbusiness/article/nyc-coolroofs, Accessed date: August 2017.

Oberndorfer, E., Lundholm, J., Bass, D., Coffman, R.R., Doshi, H., Dunnett, N., Gaffin, S., Köhler, M., Liu, K.K.Y., Rowe, B., 2007. Green roofs as urban ecosystems: ecological structures, functions, and services. Bioscience 57 (10), 823–833. http://dx.doi.org/10.1641/B571005.

Oke, T.R., 1987. Boundary Layer Climates, Second Edition. Routledge, London, UK (ISBN 0-415-04319-0).

Orlove, G.L., 2013. Emissivity Explained in Plain English. Infrared Training Center. https://www.youtube.com/watch?v=gueQrS6ORI0, Accessed date: August 2017.
PCE, 2017. Infrared Thermometer PCE-777. https://www.pce-instruments.com/us/measuring-instruments/test-meters/infrared-thermometer-pce-instruments-infrared-thermometer-pce-777-det_2183307.htm?_list=qr.art&_listpos=1, Accessed date: August 2017.
Rosenzweig, C., Solecki, W. (Eds.), 2015. New York City Panel on Climate Change 2015 Report. Ann. N. Y. Acad. Sci.http://dx.doi.org/10.1111/nyas.12591.
Synnefa, A., Santamouris, M., Livada, I., 2006. A study of the thermal performance of reflective coatings for the urban environment. Sol. Energy 80, 968–982. http://dx.doi.org/10.1016/j.solener.2005.08.005.
Takebayashi, H., Moriyama, M., 2007. Surface heat budget on green roof and high reflection roof for mitigation of urban heat island. Build. Environ. 42, 2971–2979. http://dx.doi.org/10.1016/j.buildenv.2006.06.017.
ThermoWorks, 2017. ThermoWorks IR Pro. http://www.thermoworks.com/IR-Gun?gclid=EAIaIQobChMIn_Dyzoq-1QIVk4ZpCh0S-QwoEAYYASABEgJplvD_BwE, Accessed date: August 2017.
U.S. Environmental Protection Agency (U.S. EPA), 2008. Chapter 3 - green roofs. In: Reducing Urban Heat Islands: Compendium of Strategies, . https://www.epa.gov/sites/production/files/2017-05/documents/reducing_urban_heat_islands_ch_3.pdf, Accessed date: August 2017.
Unger, J., Gál, T., Rakonczai, J., Mucsi, L., Szatmári, J., Tobak, Z., van Leeuwen, B., Fiala, K., 2009. In: Air Temperature Versus Surface Temperature in Urban Environments. Seventh International Conference on Urban Climate, Yokohama, Japan. . http://publicatio.bibl.u-szeged.hu/5899/1/375624_1_090514014110_003_u.pdf, Accessed date: August 2017.
Wang, S.K., 2001. Handbook of Air Conditioning and Refrigeration, 4.1 Indoor Design Conditions. McGraw-Hill. http://www.gmpua.com/CleanRoom/HVAC/Cooling/Handbook%20of%20Air%20Conditioning%20and%20Refrigeration.pdf, Accessed date: August 2017.
Wilbanks, T., Fernandez, S., 2013. Climate Change and Infrastructure, Urban Systems, and Vulnerabilities: Technical Report for the U.S. Department of Energy in Support of the National Climate Assessment. Island Press, Washington, DC. https://link.springer.com/content/pdf/10.5822/978-1-61091-556-4.pdf, Accessed date: August 2017.